

# Influence of pump power and beam diameter on the transverse relaxation rate of noble gas nuclear spins in the nuclear magnetic resonance gyroscope

Mao Yunkai<sup>a</sup>, Dong Boxian<sup>a</sup>, Li Jianli<sup>a,b</sup>, Liu Zhanchao<sup>a,b</sup>, and Jie Shaofeng<sup>a</sup>

<sup>a</sup>School of Instrumentation and Optoelectronic Engineering, Beihang University, Xueyuan Road No. 37, Haidian District, Beijing, 100191, China

<sup>b</sup>Beihang Hangzhou Innovation Institute Yuhang, Xixi Octagon City, Yuhang District, Hangzhou 310023, China

## ABSTRACT

Nuclear magnetic resonance gyroscopes (NMRGs) have broad application perspectives with the advantages of low cost, low power consumption, miniaturization-ability and high precision. The transverse relaxation rate of noble gas nuclear spins is used to evaluate the performance of vapor cell, which also affects the angle random walk (ARW) of NMRG systems. The inhomogeneity of electronic spin polarization spatial distribution is one of the essential sources of the transverse relaxation rate. In this paper, we study the influence of the pump power and beam diameter in the transverse relaxation rate of noble gas nuclear spins through numerical simulations of electronic spin polarization and experimental measurements of transverse relaxation time. Simulations of the electronic spin polarization spatial distribution are proposed based on the Bloch–Torrey equations. The transverse relaxation time of noble gas nuclear spins under different pump power and beam diameters is measured by the free induction decay (FID) method. Experimental results show that the transverse relaxation rate of nuclear spins increases with pump power. The relaxation rate with a 2.3mm pump beam diameter is larger than with a 1.3mm diameter. Furthermore, we innovatively find that the transverse relaxation rate shows a linear relationship with the electronic spin polarization obtained from the numerical simulation. This work provides a reference for the study of nuclear spin relaxation and the optimization of the parameters of the pump beam in NMRGs.

**Keywords:** pump power, pump beam diameter, electronic spin polarization, transverse relaxation rate, nuclear magnetic resonance gyroscope

## 1. INTRODUCTION

Atomic sensors play a significant role in many areas, such as magnetic field measurement<sup>1,2</sup> and inertial measurement.<sup>3,4</sup> NMRGs are gaining more and more attention as a typical kind of micro atomic sensors with the advantages of low cost and high precision.<sup>5,6</sup> The transverse relaxation time of noble gas nuclear spins affects the angle random walk (ARW), and it is considered to be an important parameter to evaluate the performance of NMRGs.<sup>3</sup> Therefore, the study of transverse relaxation rate has become an essential issue.

Laser parameters have effects on the performance of atomic sensors, while pump power and beam diameter especially affect the spatial distribution of electronic spin polarization.<sup>7–9</sup> Researchers have analyzed the spatial distribution of electronic spin polarization through the numerical simulation method.<sup>9,10</sup> The inhomogeneity of electronic spin polarization has a significant effect on signal amplitude and measurement accuracy.<sup>11</sup> In NMR gyroscopes, the inhomogeneity of electronic spin polarization would affect the inertial measurement sensitivity.<sup>9</sup> However, these research findings need to include the analysis of the influence of laser parameters on transverse relaxation time.

---

Further author information: (Send correspondence to Li Jianli)

Li Jianli: E-mail: lijianli@buaa.edu.cn

Mao Yunkai: E-mail: maoyunkai6@buaa.edu.cn

In this paper, the influence of pump power and beam diameter on the transverse relaxation time in the NMRG is analyzed. Firstly, the spatial distribution of electronic spin polarization under different pump power and beam diameters is simulated based on the Bloch-Torrey equations. Then the transverse relaxation time of noble gas nuclear spins is measured through the FID method. Finally, the correlation between the average electronic spin polarization and the transverse relaxation rate of noble gas nuclear spins is obtained, which is of great significance for the study of the composition of the transverse relaxation rate and the improvements in the accuracy of NMRGs.

## 2. PRINCIPLE

### 2.1 Numerical simulations of the electronic spin polarization

In the NMRGs, the electronic spin polarization spatial distribution satisfies the Bloch-Torrey equations:<sup>12</sup>

$$\frac{\partial \mathbf{P}_e}{\partial t} = \gamma_e \mathbf{P}_e \times \mathbf{B} + D_e \nabla^2 \mathbf{P}_e + R_{op}(1 - P_e) - R_e \mathbf{P}_e, \quad (1)$$

where  $\mathbf{P}_e$  represents the spin polarization of the alkali metal electrons,  $D_e$  represents the diffusion of the alkali metal electrons,  $\gamma_e$  is gyromagnetic ratio,  $R_{op}$  indicates the rate of optical pumping, the total relaxation rate of alkali metal electrons is  $R_e$ . The value of these parameters could refer to Jia's research.<sup>9</sup>

Under the steady-state condition, this equation can be simplified into:

$$D_e \nabla^2 \mathbf{P}_e = R_e \mathbf{P}_e - R_{op}(1 - \mathbf{P}_e), \quad (2)$$

The boundary condition of equation(2) is:

$$D_e \nabla \mathbf{P}_e = \mathbf{P}_e (R_{op} D_e)^{(-1/2)}. \quad (3)$$

### 2.2 The FID method in measuring the transverse relaxation time

The transverse relaxation time of atoms is measured through the FID method, which is the industry standard method. Taking the magnetic field and relaxation time into consideration, the net magnetization vector of noble gas satisfies the Bloch equations:<sup>13</sup>

$$\begin{cases} \frac{dM_x}{dt} = \gamma_n (M_y B_z - M_z B_y) - \frac{M_x}{T_2} \\ \frac{dM_y}{dt} = \gamma_n (M_z B_x - M_x B_z) - \frac{M_y}{T_2} \\ \frac{dM_z}{dt} = \gamma_n (M_x B_y - M_y B_x) - \frac{M_0 - M_z}{T_1} \end{cases}, \quad (4)$$

where  $T_1$  represents the longitudinal relaxation time, and  $T_2$  represents the transverse relaxation time,  $M_x$ ,  $M_y$ , and  $M_z$  respectively indicate the projection of the net magnetization vector along the  $x$ ,  $y$ ,  $z$  direction,  $\gamma_n$  indicates the gyromagnetic ratio of noble gas Xe.

The FID method requires a  $\pi/2$  pulse to drive up the Xe precession. The driven magnetic field and duration time are expressed as:

$$\gamma_n \frac{B_1}{2} t_{\pi/2} = \frac{\pi}{2}, \quad (5)$$

where  $B_1$  is the driven magnetic field and  $t_{\pi/2}$  is the duration time of the pulse.

When the pulse is applied, the magnetic field becomes into:

$$\begin{cases} B_x = B_1 \cos(\omega_a t) \\ B_y = B_1 \sin(\omega_a t) \\ B_z = B_0 \end{cases} \quad 0 < t \leq t_{\pi/2}, \quad (6)$$

where  $\omega_a$  represents the frequency of the resonance between noble gas and static magnetic field  $B_0$ , which means  $\omega_a = \gamma_n B_0$ .

When the driven magnetic field  $B_1$  is shut down, the solutions could be obtained through the equation(4):

$$\begin{cases} M_x = M_{xyt_{\pi/2}} e^{-\frac{(t-t_{\pi/2})}{T_2}} \cos(\omega_a t - \phi) \\ M_y = M_{xyt_{\pi/2}} e^{-\frac{(t-t_{\pi/2})}{T_2}} \sin(\omega_a t + \phi) \\ M_z = M_{zt_{\pi/2}} [1 - e^{-\frac{(t-t_{\pi/2})}{T_1}} (1 - \frac{M_{zt_{\pi/2}}}{M_{t_{\pi/2}}})] \end{cases} \quad t \geq t_{\pi/2}, \quad (7)$$

where  $M_{xyt_{\pi/2}}$  and  $M_{zt_{\pi/2}}$  respectively indicate the projection of the net magnetization vector on the  $x - y$  plane and along the  $z$  direction at  $t = t_{\pi/2}$ .

### 3. RESULTS AND DISCUSSIONS

#### 3.1 Numerical simulation results of the electronic spin polarization

The electronic spin polarization spatial distribution is obtained through the COMSOL Multiphysics software by solving the equation(2) with the boundary conditions equation(3). In the experiments, we use a cubic vapor cell with an inner length of 3mm. Therefore, 1.3mm and 2.3mm are chosen to be the beam diameters in the numerical simulations. Considering the laser power range of the pump laser in the microfabricated NMRGs, the power range in the simulations is set to be 0.5mW to 5mW.

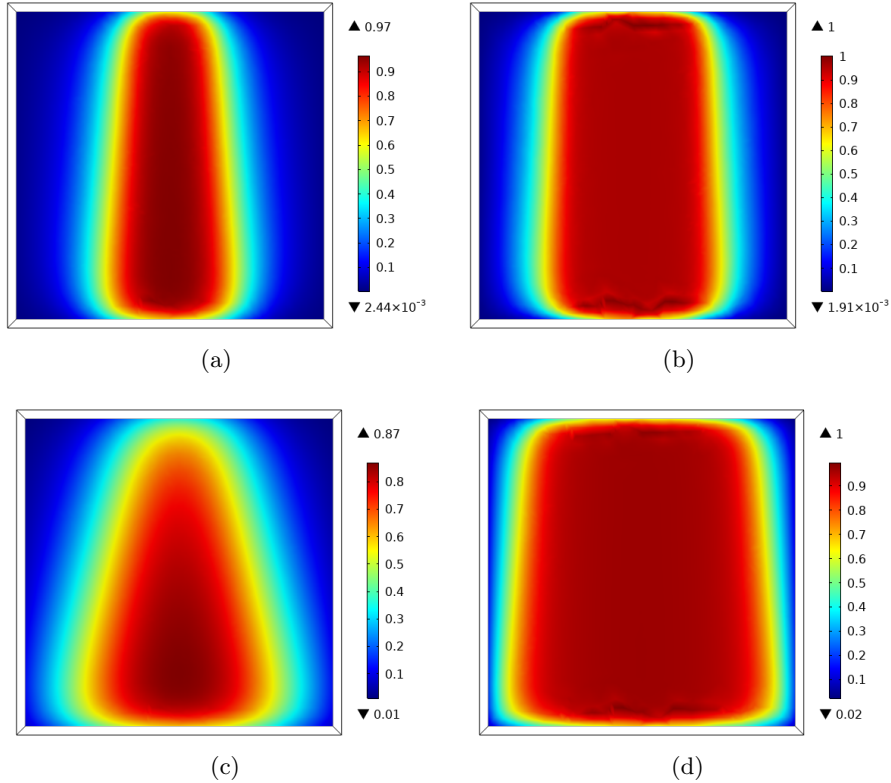


Figure 1. The spatial distribution of the electronic spin polarization in the  $y$ - $z$  plane .(a)0.5mW pump power and 1.3mm beam diameter (b)4mW pump power and 1.3mm beam diameter(c)0.5mW pump power and 2.3mm beam diameter (d)4mW pump power and 2.3mm beam diameter

Fig.1 shows the spatial distribution of electronic spin polarization under different pump power and beam diameters. It can be seen that the pump power and beam diameter have a significant impact on the inhomogeneity of the electronic spin polarization, but it is difficult to be described accurately and quantitatively. The average spin polarization increases with the pump power, and the increasing speed decreases with the pump power.

Moreover, Fig.2 illustrates the relationship between the average spin polarization and pump power. The maximum average spin polarization under different diameters seems to be limited. The average spin polarization with the 1.3mm and 2.3 mm beam diameters is 0.3427 and 0.6194, when the pump power is 5mW. The ratio of the pump power is 1.81 while the ratio of beam diameters is 1.76, so the limits of the maximum average spin polarization may have a linear relationship with the beam diameter, which is an interesting observation.

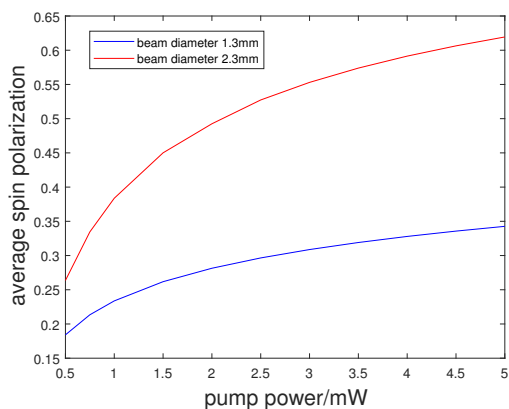


Figure 2. Average spin polarization

### 3.2 Experimental measurements of $T_2$

The experiment setup is shown in Fig.3. The pump laser has the same direction as the static magnetic field

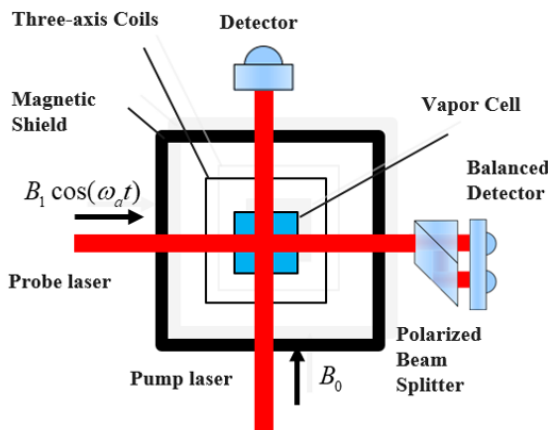


Figure 3. A schematic of the experimental setup

$B_0$ , whose wavelength is at the D1 line of Rb. The probe laser has the same direction as the driving magnetic field, and its wavelength is at the D2 line of Rb. After passing through the vapor cell, the probe laser passes through the spin polarization beam splitter and is detected by the balance detector. The pump laser is circularly polarized while the probe laser is linear polarized. The outer length of the cubic vapor cell is 4mm, and the wall thickness is 0.5mm. The composition of the vapor cell is natural abundance Rb, 2 Torr  $^{129}\text{Xe}$ , 8 Torr  $^{131}\text{Xe}$  and 200 Torr  $\text{N}_2$ . The electronic heater with magnetic field suppression function heats the vapor cell to  $110^\circ\text{C}$ . The magnetic shielding system is used to suppress the interference of the environmental magnetic field, and the three-axis coils are used to generate the magnetic field required by NMRGs.

Experimental results show that the transverse relaxation time decreases with the increase of pump power, and the attenuation speed also decreases with the increase of pump power in Fig.4(a). Under the same pump power condition, the relaxation time with a 2.3mm pump beam diameter is shorter than with a 1.3mm pump beam

diameter. It is worth noting that in Fig.4(b), we innovatively find the transverse spin relaxation rate shows a linear relationship with the average electronic spin polarization, which is obtained through the numerical simulations. The goodness of fit with the 1.3mm beam diameter and the 2.3mm beam diameter is 0.9954 and 0.9904, respectively. The transverse relaxation rate of noble gas nuclear spins  $\Gamma$  in the NMRGs consists of these

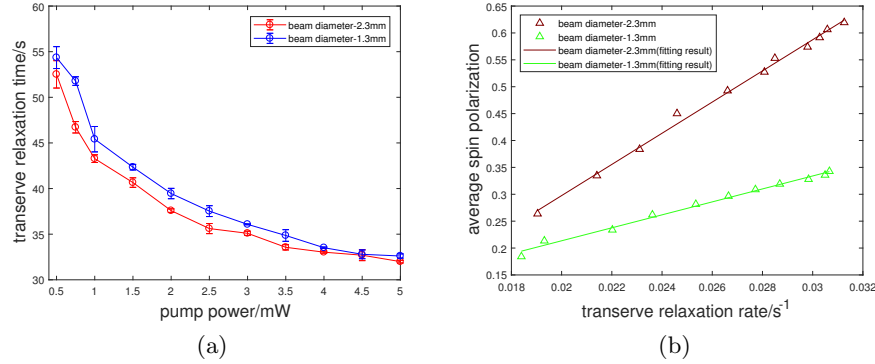


Figure 4. The influence of pump beam and beam diameter in the transverse relaxation time. (a) the transverse relaxation time under different pump laser parameters (b) the relationship between the transverse relaxation rate and the electronic spin polarization

following parts:<sup>14</sup>

$$\Gamma = \Gamma_{coll} + \Gamma_{wall} + \Gamma_{\Delta B} + \Gamma', \quad (8)$$

where  $\Gamma_{coll}$  represents the relaxation rate caused by collisions between noble gas and Rb atoms,  $\Gamma_{wall}$  represents the relaxation rate caused by the collisions between noble gas atoms and the cell wall,  $\Gamma_{\Delta B}$  represents the relaxation rate caused by the magnetic field inhomogeneity, and  $\Gamma'$  represents the relaxation rate caused by the self-collisions of noble gas atoms.

The  $\Gamma_{coll}$  is proportional to the density of Rb atoms,<sup>14</sup> and the density of the polarized Rb atoms can be considered to be positively related to the average polarization. Therefore, one of the sources of influence on the transverse relaxation rate from the pump laser may be the average electronic spin polarization.

On the other hand, the Rb magnetic field sensed by the noble gas can be expressed as:<sup>4,15</sup>

$$B_{Rb} = K P_e, \quad (9)$$

where  $K$  is a scalar parameter, which is proportional to the enhancement factor of Rb–Xe interaction, the electron moment and the Rb density. According to the equation (9), the inhomogeneity of the alkali-metal vector magnetic field is considered to be caused by the inhomogeneity of the electronic spin polarization spatial distribution.

In conclusion, the pump laser can affect the transverse relaxation rate through its effect on the magnetic field inhomogeneity and the collisions between noble gas and alkali metal atoms. This theoretical analysis has the potential to be the effective explanation for the experimental results shown in Figure. (4). The quantitative contribution of the pump lasers parameters to the two components of the relaxation rate is worthy of further study.

#### 4. CONCLUSION

Focusing on the influence of the pump beam parameters on the transverse relaxation rate of noble gas nuclear spins in the NMRGs, we simulate the electronic spin polarization spatial distribution in three-dimensional space and measure the transverse relaxation time of noble gas nuclear spins. It is concluded that pump power and beam diameter obviously affect the electronic spin polarization spatial distribution and average electronic spin polarization. Meanwhile, the transverse relaxation rate of noble gas nuclear spins increases with pump power, and the transverse relaxation rate is larger under a larger pump beam diameter. Moreover, the transverse relaxation rate shows a linear relationship with the average electronic spin polarization. This work provides a reference for the study of nuclear spin relaxation and optimization of the parameters of the pump laser in NMRGs.

## ACKNOWLEDGMENTS

This work was supported by National Key Research and Development Program of China (2018YFB2002404) and The National Natural Science Foundation of China Youth Fund (61722103).

## REFERENCES

- [1] Shah, V. and Romalis, M. V., “Spin-exchange relaxation-free magnetometry using elliptically polarized light,” *Physical Review A* **80**(1), 013416 (2009).
- [2] Sheng, D., Kabcenell, A., and Romalis, M. V., “New classes of systematic effects in gas spin comagnetometers,” *Physical review letters* **113**(16), 163002 (2014).
- [3] Eklund, E. J., [*Microgyroscope based on spin-polarized nuclei*] (2008).
- [4] Walker, T. G. and Larsen, M. S., “Spin-exchange-pumped NMR gyros,” in [*Advances in atomic, molecular, and optical physics*], **65**, 373–401 (2016).
- [5] Gundeti, V. M., [*Folded MEMS approach to NMRG*] (2015).
- [6] Noor, R. M. and Shkel, A. M., “MEMS components for NMR atomic sensors,” *Journal of Microelectromechanical Systems* **27**(6), 1148–1159 (2018).
- [7] Chen, L., Lei, G., Wu, W., Hong, J., and Zhou, B., “The optimal frequency and power of a probe beam for atomic sensor,” in [*AOPC 2015: Advances in laser technology and applications*], **9671**, 366–371 (2015).  
tex.organization: SPIE.
- [8] Duan, L., Fang, J., Li, R., Jiang, L., Ding, M., and Wang, W., “Light intensity stabilization based on the second harmonic of the photoelastic modulator detection in the atomic magnetometer,” *Optics Express* **23**(25), 32481–32489 (2015).
- [9] Yuchen, J., Zhanchao, L., Binqian, Z., Xiaoyang, L., Wenfeng, W., Jinpeng, P., Ming, D., Yueyang, Z., and Jiancheng, F., “Pump beam influence on spin polarization homogeneity in the nuclear magnetic resonance gyroscope,” *Journal of Physics D: Applied Physics* **52**(35), 355001 (2019).
- [10] Ito, Y., Ohnishi, H., Kamada, K., and Kobayashi, T., “Effect of spatial homogeneity of spin polarization on magnetic field response of an optically pumped atomic magnetometer using a hybrid cell of K and Rb atoms,” *IEEE transactions on magnetics* **48**(11), 3715–3718 (2012).
- [11] Ito, Y., Sato, D., Kamada, K., and Kobayashi, T., “Optimal densities of alkali metal atoms in an optically pumped K–Rb hybrid atomic magnetometer considering the spatial distribution of spin polarization,” *Optics Express* **24**(14), 15391–15402 (2016).
- [12] Grebenkov, D. S., “NMR survey of reflected Brownian motion,” *Reviews of Modern Physics* **79**(3), 1077 (2007).
- [13] Franzen, W., “Spin relaxation of optically aligned rubidium vapor,” *Physical Review* **115**(4), 850 (1959).
- [14] Liu, X., Chen, C., Qu, T., Yang, K., and Luo, H., “Transverse spin relaxation and diffusion-constant measurements of spin-polarized  $^{129}\text{Xe}$  nuclei in the presence of a magnetic field gradient,” *Scientific reports* **6**(1), 1–8 (2016).
- [15] Zhan, X., Chen, C., Wang, Z., Jiang, Q., Zhang, Y., and Luo, H., “Improved compensation and measurement of the magnetic gradients in an atomic vapor cell,” *AIP Advances* **10**(4), 045002 (2020).